

METALS  
AND SUPERCONDUCTORS

# Effect of Heterovalent Substitution of Rare-Earth Elements on the Magnetic and Transport Properties of $\text{YBa}_2\text{Cu}_3\text{O}_7$

M. I. Petrov, D. A. Balaev, Yu. S. Gokhfel'd, A. A. Dubrovskii, and K. A. Shaikhutdinov

*Kirensky Institute of Physics, Siberian Branch, Russian Academy of Sciences, Krasnoyarsk, 660036 Russia*

*e-mail: smp@iph.krasn.ru*

Received February 20, 2007

**Abstract**—The  $\text{Y}_{(1-x)}\text{Ce}_x\text{Ba}_2\text{Cu}_3\text{O}_7$  system with low cerium concentrations has been synthesized. The cerium solubility limit measured using x-ray powder diffraction analysis is about 2.4 at. %. The temperature dependences of the magnetization  $M(T)$  are measured for samples cooled in a magnetic field (FC) and in a zero field (ZFC). The difference between the magnetizations  $M_{\text{ZFC}} - M_{\text{FC}}$  at 77.4 K, which is proportional to the pinning potential, passes through a maximum at  $x = 0.0156$ . This concentration corresponds to the average distance (equal to eight lattice constants) between the impurity ions in the plane of the rare-earth elements, which is comparable to the diameter of Abrikosov vortices in  $\text{YBa}_2\text{Cu}_3\text{O}_7$ .

PACS numbers: 74.25.Qt, 74.62.Dh, 74.72.Bk

DOI: 10.1134/S1063783407110054

## 1. INTRODUCTION

Superconductors of the Y-123 family incorporating rare-earth elements (i.e.,  $\text{R}\text{Ba}_2\text{Cu}_3\text{O}_7$ , where  $R$  stands for a rare-earth element) are presently the best studied and most promising materials for emerging applications. That is why the increase in the critical current density is an urgent issue. One of the ways to reach this goal lies in creating pinning centers in the grains. Non-superconducting regions in the sample, which can be formed by various means, can act as pinning centers. One of these means consists in doping the crystal lattice by different cations.

Many researchers had studied the effect of doping by various rare-earth elements introduced in different combinations on the properties of  $\text{YBa}_2\text{Cu}_3\text{O}_7$  (YBCO). Most of the rare-earth elements doped onto yttrium sites affect only weakly the critical temperature and the critical current [1]. Cerium cannot form the 123 structure and, when doped, precipitates as a nonsuperconducting phase [2]. The effect of rare-earth impurities on YBCO properties was studied for concentrations of about a few tens of atomic percents [3–10], which, in our opinion, does not permit investigation of lattice point distortions on the superconducting properties. Study of the effect of low dopant concentrations on the magnetic and transport properties should permit a better insight into the mechanism of pinning in YBCO-based superconductors doped by oxides of rare-earth elements.

Impurities introduced in small amounts into a superconductor can either dissolve in the lattice to form point defects through distortion of the electronic structure or precipitate in nanosized inclusions of nonsupercon-

ducting phases [11]. In order to identify the origin of pinning centers, one has to investigate the effect of impurity concentration on the properties of grains and intergrain space.

The present paper reports on an experimental study of the magnetic and transport characteristics of the yttrium HTSC system  $\text{Y}_{(1-x)}\text{Ce}_x\text{Ba}_2\text{Cu}_3\text{O}_7$ , in which yttrium ions were substituted for by ions of cerium in different concentrations. We chose the concentration  $x$  such that the most probable distance between cerium ions is a multiple of the lattice constant in the plane, i.e.,  $x = 1/n^2$ , where  $n = 2, 3, 4, 5, 6, 7, 8, 9, 10$ , and  $\infty$ . This was done under the assumption that cerium atoms occupy yttrium sites and are uniformly distributed over the rare-earth plane (Fig. 1). The composition of a sample with  $n = \infty$  corresponds to classical  $\text{YBa}_2\text{Cu}_3\text{O}_7$ .

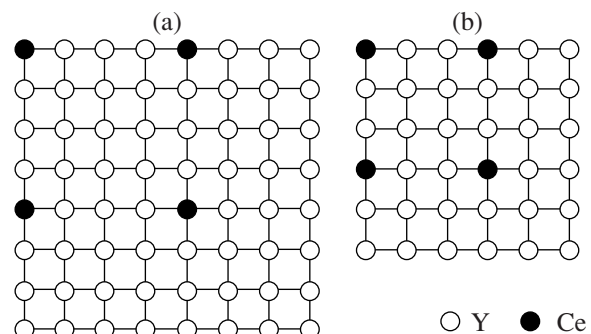


**Fig. 1.** Idealized lattice in the plane of rare-earth elements in the (123) structure for (a)  $n = 4$ ,  $x = 0.0625$  and (b)  $n = 3$ ,  $x = 0.11$ .

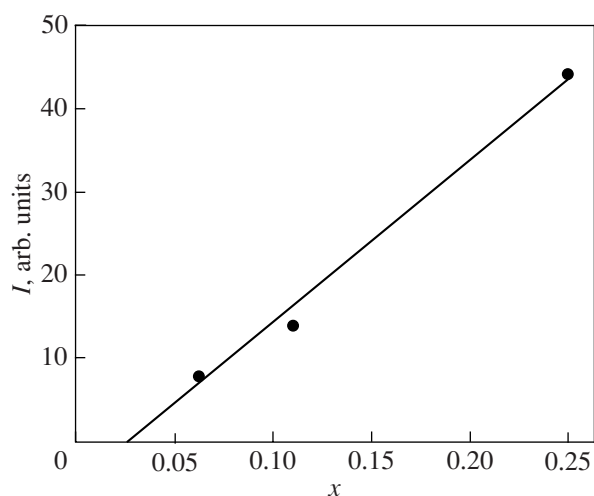


**Fig. 2.** Dependence of the maximum relative intensity of diffraction reflections from  $\text{BaCeO}_3$  on the Ce content in the  $\text{Y}_{(1-x)}\text{Ce}_x\text{Ba}_2\text{Cu}_3\text{O}_7$  compounds.

## 2. EXPERIMENT

Ten samples of  $\text{Y}_{(1-x)}\text{Ce}_x\text{Ba}_2\text{Cu}_3\text{O}_7$  with  $x = 0.25, 0.11, 0.0625, 0.04, 0.0278, 0.0204, 0.0156, 0.0123, 0.01,$  and  $0$ , which corresponds to  $n = 2, 3, 4, 5, 6, 7, 8, 9, 10,$  and  $\infty$ , were synthesized by the standard solid-phase technique. The starting reactants were  $\text{Y}_2\text{O}_3, \text{CeO}_2,$  and  $\text{CuO}$  (reagent grade) and  $\text{BaCO}_3$  (analytical grade).

The corresponding amounts of reagents were mixed thoroughly in an agate mortar, pelletized, and annealed at  $930^\circ\text{C}$ . The synthesis, including seven intermediate crushings and pressings, lasted 160 h. Longer procedures favor ordering of rare-earth elements and cerium substitution in yttrium positions. The synthesis completed, the samples were annealed at a temperature of  $300^\circ\text{C}$  for 3 h and cooled slowly in the furnace to room temperature to reach oxygen saturation.

The electrical resistivity was measured by the standard four-point probe technique with samples of rectangular cross section ( $\approx 2 \times 1$  mm), the distance between the potential contacts being 2 mm.

The magnetic properties were measured with a vibrating-sample magnetometer [12]. The samples were cut out in the shape of cylinders  $\approx 5$  mm in height and  $\approx 0.5$  mm in diameter. The magnetic field was applied parallel to the cylinder axis.

## 3. RESULTS AND DISCUSSION

Because cerium cannot form 123-type structures [2], its solubility in the YBCO lattice should not be high. At low cerium concentrations ( $<5\%$ ) in  $\text{Y}_{(1-x)}\text{Ce}_x\text{Ba}_2\text{Cu}_3\text{O}_7$ , the determination of the fraction of a foreign phase by the x-ray powder diffraction analysis meets with difficulties. Therefore, we performed the x-ray powder diffraction analysis of the samples

with cerium contents of 0.25, 0.11, and 0.0625. The dependence of the reflection intensity of the foreign phase  $\text{BaCeO}_3$  on the cerium concentration is presented in Fig. 2. To estimate the solubility limit of cerium in the YBCO structure, we extrapolated the data obtained with a straight line. The solubility of cerium was found to be about 2.4 at. %.

The temperature dependences of the electrical resistivity  $\rho(T)$  were measured for all the  $\text{Y}_{(1-x)}\text{Ce}_x\text{Ba}_2\text{Cu}_3\text{O}_7$  samples. Figure 3 displays the dependences  $\rho(T)$  for samples with  $x = 0.25, 0.11, 0.0156,$  and  $0$ . Above the transition temperature  $T_c$ , all the dependences have metallic character. The ratio  $\rho(300 \text{ K})/\rho(100 \text{ K})$  decreases, however, monotonically with increasing cerium concentration (Fig. 4a). Data on the cerium concentration in Fig. 4 are given in units of  $n$  ( $x = 1/n^2$ ).

The electrical resistivity does not practically change in magnitude (within the accuracy of the measurement of the cross-sectional area of the samples) for compositions with  $x$  varying from 0 to 0.0625 and at 300 K is about  $3.0 \times 10^{-3} \Omega \text{ cm}$ . The electrical resistivity of samples with higher cerium concentrations increases to become about 0.01 and  $0.12 \Omega \text{ cm}$  for compositions with  $x = 0.11$  and 0.25, respectively.

The resistive transition in the samples under study is typical of granular HTSCs [13–15] and exhibits a sharp drop of the resistance at  $T_c$  and a smooth part. The insets to Fig. 3 present the dependences  $\rho(T)$  in the region of the superconducting transition. The sharp jump in the resistivity occurring at  $T_c$  can be identified with the transition in HTSC grains [13–15]. The values of  $T_c$  coincide with the critical temperatures derived from magnetic measurements. The temperatures  $T_c$  obtained in this way are practically independent of the cerium content in the sample and vary within 91–92 K. The lowest value  $T_c = 90.8 \text{ K}$  was obtained in the sample with  $x = 0.25$ . The smooth part in  $\rho(T)$  can be assigned to the transition at intergrain boundaries, which in granular HTSCs are Josephson weak links [13–15]. This part of  $\rho(T)$  broadens with increasing transport current, a feature observed by us in samples of this lot under application of a magnetic field as well [13, 15]. The temperature range in  $\rho(T)$  corresponding to the transition at intergrain boundaries can be taken as a characteristic of the “strength” of Josephson links in granular HTSCs. Figure 4b plots the width of this temperature range  $\Delta T = T_c - T_c(R = 0)$  as a function of  $n$  ( $x = 1/n^2$ ); here,  $T_c(R = 0)$  is the temperature at which the sample resistance vanishes. The width of the superconducting transition  $\Delta T$  is  $2^\circ\text{--}4^\circ$  for compositions with  $x$  varying from 0 to 0.04. As  $x$  increases,  $\Delta T$  is observed to increase markedly. For the composition with  $x = 0.25$ ,  $T_c(R = 0)$  is about 78 K. The above analysis of the dependences  $\rho(T)$  suggests that, at cerium concentrations above 0.0625 ( $n = 4$ ), Josephson links weaken substantially. This conforms to the x-ray powder dif-

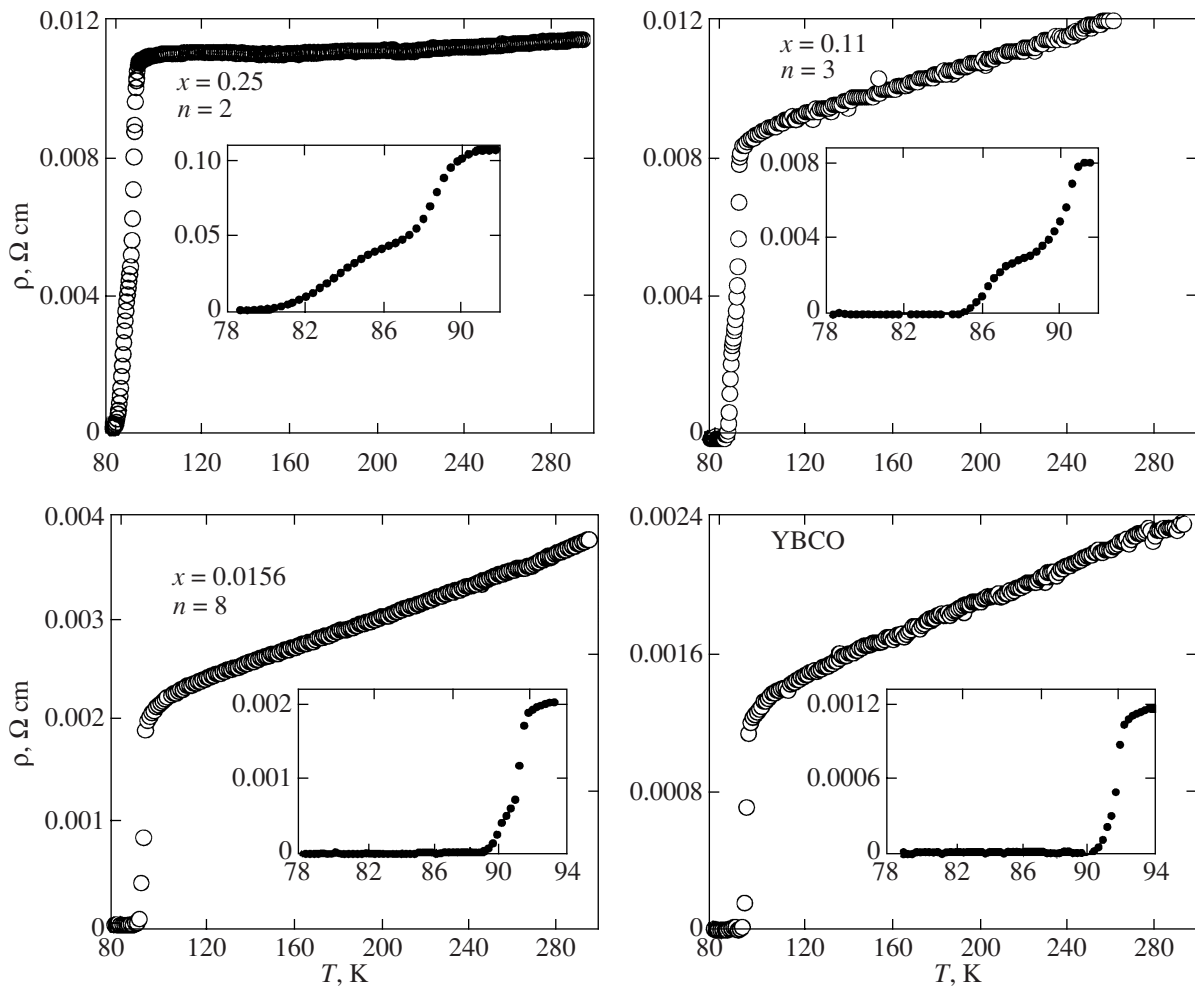


**Fig. 3.** Temperature dependences of the electrical resistivity  $\rho(T)$  of  $Y_{(1-x)}Ce_xBa_2Cu_3O_7$  samples. The insets show the dependence  $\rho(T)$  in the region of the resistive transition.

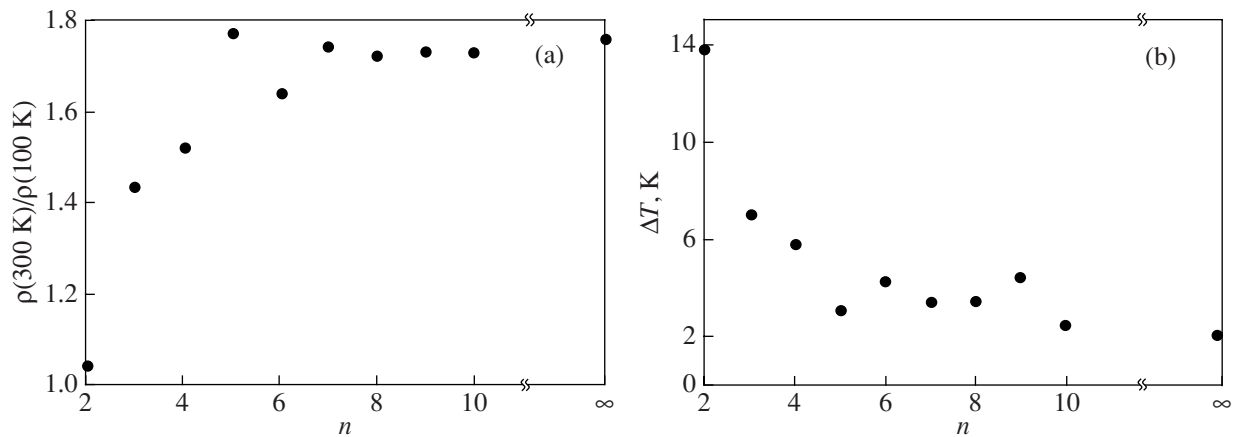


**Fig. 4.** (a) Dependences of the ratio  $\rho(300\text{ K})/\rho(100\text{ K})$  and (b) the superconducting transition width on the cerium content in the  $Y_{(1-x)}Ce_xBa_2Cu_3O_7$  compounds.

fraction data obtained for these samples (Fig. 2), which indicate the formation of the second phase ( $BaCeO_3$ ). It is known that the formation of a nonsuperconducting

phase reduces the “strength” of Josephson links in granular HTSCs, which, in this case, are already two-phase composites. For compositions with  $x \leq 0.0625$ ,

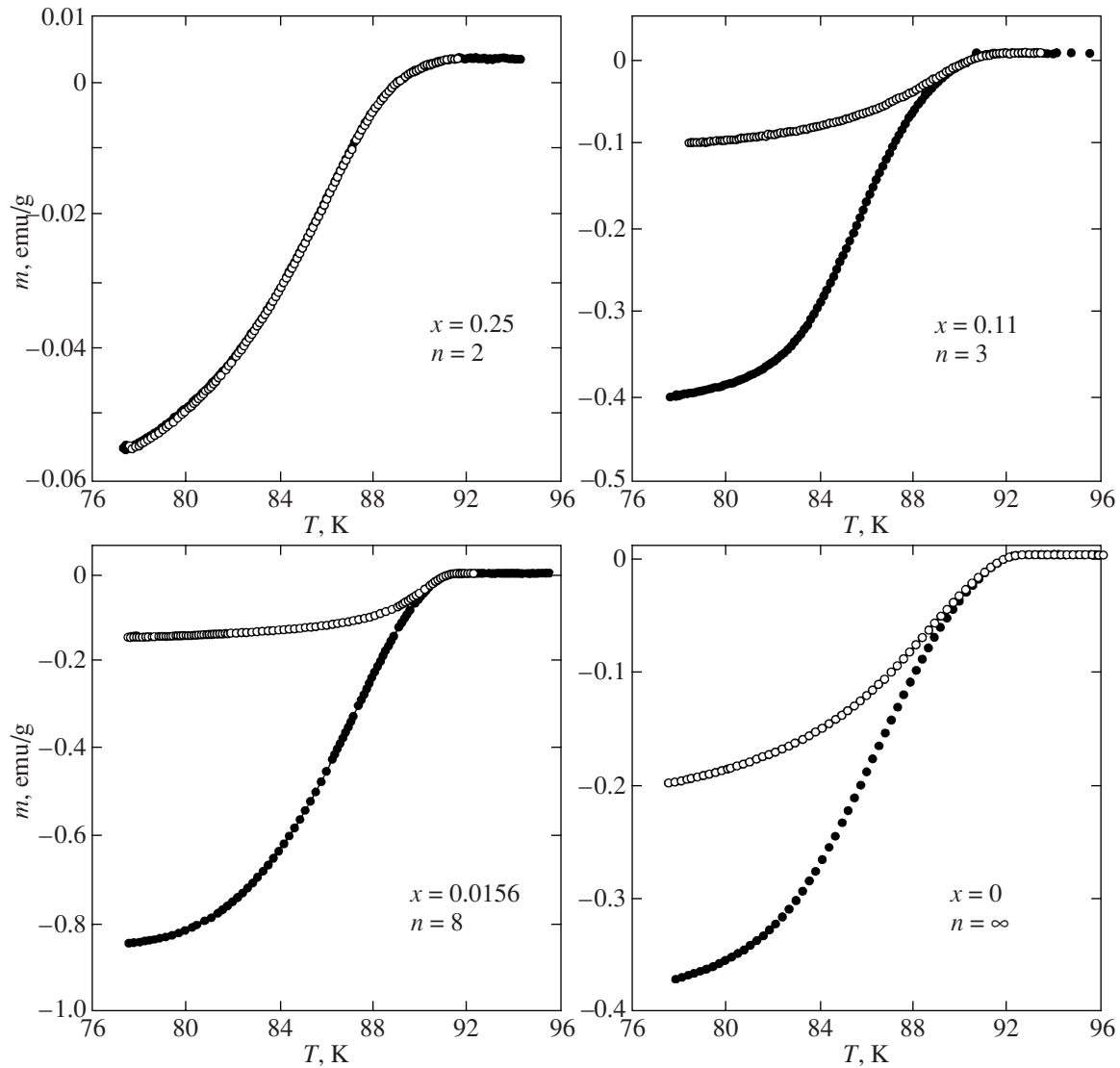


Fig. 5. Temperature dependences of the magnetizations  $M_{FC}$  (open circles) and  $M_{ZFC}$  (closed circles) in the field  $H = 100$  Oe.

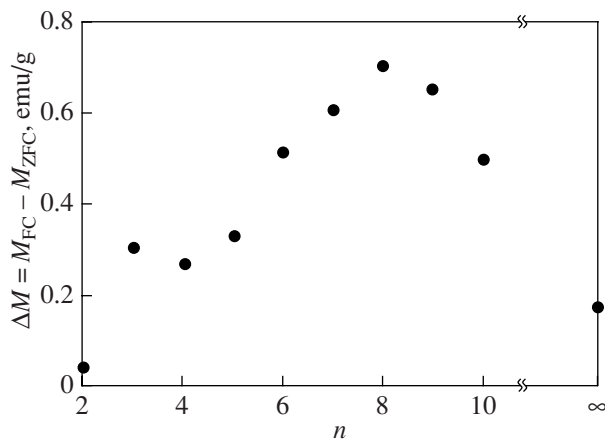


Fig. 6. Difference between the magnetic moments of the field-cooled ( $M_{FC}$ ) and zero-field-cooled ( $M_{ZFC}$ ) samples at  $T = 77.4$  K.

such parameters as  $T_c$ ,  $\rho(300\text{ K})$ ,  $\rho(300\text{ K})/\rho(100\text{ K})$ , and  $\Delta T$ , practically do not differ from those measured in  $\text{YBa}_2\text{Cu}_3\text{O}_7$ .

In order to establish the effect of the cerium content on the intragrain pinning in  $\text{Y}_{(1-x)}\text{Ce}_x\text{Ba}_2\text{Cu}_3\text{O}_7$ , we measured the temperature dependences of the magnetization  $M(T)$  of the samples. The difference between the field-cooled and zero-field-cooled sample magnetizations  $M_{FC}$  and  $M_{ZFC}$  is known to be proportional to the pinning force and, hence, to the critical current [16]. Figure 5 plots the temperature dependences of the magnetizations  $M_{FC}$  and  $M_{ZFC}$  for samples with  $x = 0.25$ , 0.11, 0.0156, and 0. Figure 6 displays the dependence of the difference between the magnetizations  $\Delta M = M_{FC} - M_{ZFC}$  as a function of  $n$  at 77 K. This curve passes through a clearly pronounced maximum at  $n = 8$  ( $x = 0.0156$ ). The major contribution to the magnetization

measured in a constant field comes from the grains, which implies that the diamagnetic response is governed by intragrain currents. This gives grounds to interpret the above observation as a result of the increase in the intragrain critical current density. In samples with a low cerium content, the impurity Ce atoms (valence state  $> +3$ ) act as point lattice defects and produce additional pinning centers, which favors an increase in the critical current. The most probable distance between Ce impurity atoms corresponding to the maximum pinning force is 30 Å, which is close to 1–2 coherence lengths in YBCO [17, 18]. This can find explanation in that the defects spaced at distances equal to the Abrikosov vortex diameter promote an increase in the pinning force in weak fields.

#### 4. CONCLUSIONS

Thus, the investigation of the transport and magnetic properties of a series of  $Y_{(1-x)}Ce_xBa_2Cu_3O_7$  compounds has showed that doping of cerium impurity atoms in small amounts up to the solubility limit brings about the formation of pinning centers and an increase in the intragrain critical current in the samples.

#### ACKNOWLEDGMENTS

This study was supported by the Siberian Division of the Russian Academy of Sciences (complex integration project no. 3.4), the Russian Academy of Sciences within the program “Quantum Macrophysics” (project no. 3.4), the Lavrent’ev Competition of Young Scientists of the Siberian Division of the Russian Academy of Sciences 2006 (project no. 52), and the Russian Science Support Foundation.

#### REFERENCES

1. P. H. Hor, R. L. Meng, Y. Q. Wang, L. Gao, Z. J. Huang, J. Bechtold, K. Forster, and C. W. Chu, *Phys. Rev. Lett.* **58**, 1891 (1987).

2. J. Hauck, K. Bickman, and K. Mika, *Supercond. Sci. Technol.* **11**, 63 (1998).
3. P. K. Nayak and S. Ravi, *Supercond. Sci. Technol.* **19**, 1209 (2006).
4. M. T. Weller, J. R. Grasmeder, P. C. Lanchester, and C. E. Meats, *J. Phys. F: Met. Phys.* **18**, L95 (1988).
5. K. M. Pansuria, D. G. Kuberkar, G. J. Baldha, and R. G. Kulkarni, *Supercond. Sci. Technol.* **12**, 579 (1999).
6. N. Hari Babu, M. Kambara, E. S. Reddy, Y. Shi, and D. A. Cardwell, *Supercond. Sci. Technol.* **18**, S38 (2005).
7. T. Harada and K. Yoshida, *Physica C (Amsterdam)* **383**, 48 (2002).
8. L. M. Paulius, C. C. Almasan, and M. B. Maple, *Phys. Rev. B: Condens. Matter* **47**, 11627 (1993).
9. S. Nariki, N. Sakai, M. Merakami, and I. Hirabayashi, *Physica C (Amsterdam)* **426–431**, 602 (2005).
10. L. Shi, Y. Huang, W. Pang, X. Liu, L. Wang, X. G. Li, G. Zhou, and Yuheng Zhang, *Physica C (Amsterdam)* **282–287**, 1021 (1997).
11. L. Shlyk, K. Nenkov, G. Krabbes, and G. Fuchs, *Physica C (Amsterdam)* **423**, 22 (2005).
12. A. D. Balaev, Yu. V. Boyarshinov, M. I. Karpenko, and B. P. Khrustalev, *Prib. Tekh. Éksp.*, No. 3, 167 (1985).
13. M. A. Dubson, S. T. Herbet, J. J. Calabrese, D. C. Harris, B. R. Patton, and J. C. Garland, *Phys. Rev. Lett.* **60**, 1061 (1988).
14. C. Gaffney, H. Petersen, and R. Bednar, *Phys. Rev. B: Condens. Matter* **48**, 3388 (1993).
15. A. D. Balaev, S. I. Popkov, K. A. Shaikhutdinov, and M. I. Petrov, *Fiz. Tverd. Tela (St. Petersburg)* **48** (5), 780 (2006) [*Phys. Solid State* **48** (5), 826 (2006)].
16. A. P. Malozemoff, in *Physical Properties of High-Temperature Superconductors*, Ed. by D. M. Ginzberg (Mir, Moscow, 1990), p. 87 [in Russian].
17. L. P. Gor’kov and N. B. Kopnin, *Usp. Fiz. Nauk* **156** (9), 117 (1988) [*Sov. Phys. Usp.* **31** (9), 850 (1988)].
18. D. Larbalestier, A. Gurevich, D. M. Feldmann, and A. Polyanskii, *Nature (London)* **414**, 368 (2001).

*Translated by G. Skrebtsov*